Journal of Nonlinear Optical Physics & Materials
Vol. 26, No. 1 (2017) 1750002 (17 pages)

DOI: 10.1142/S0218863517500023

Incoherently coupled photorefractive spatial solitons supported by pyroelectric effects

Aavishkar Katti* and R. A. Yadav†

Department of Physics, Institute of Science
Banaras Hindu University
Varanasi-221005 (U.P.), India
**aavishkarkatti89@gmail.com*
†*rayadav@bhu.ac.in*

Received 8 November 2016

A theory for predicting the existence of incoherently coupled spatial soliton pairs due to solely the pyroelectric effect in nonphotovoltaic–photorefractive crystals with an appreciable pyroelectric coefficient is presented. The bright–bright, dark–dark, gray–gray, and bright–dark soliton pairs are shown to exist. These soliton pairs are established if the incident beams propagate collinearly and have the same polarization and wavelength but are mutually incoherent. The magnitude of temperature change of the crystal and the incident beams' intensity profoundly affect these soliton pairs.

Keywords: Optical spatial solitons; pyroelectric effect; photorefractive crystals; incoherently coupled solitons.

1. Introduction

Solitons have been at the forefront of current research in optics. Optical solitons have potential applications in optical switching, routing and logic operations.[1–4] Fixing the optical spatial soliton results in a waveguide formation which can guide other optical beams.[5–8] There have been many other recent theoretical studies which demonstrate the diversity and richness of characteristics of optical solitons.[9–15]

Amongst the optical spatial solitons, photorefractive solitons are quite attractive because of generation at low laser powers, typically of the order of a few mW.[16] Photorefractive materials exhibit a saturable nonlinearity and hence, can support steady state optical spatial solitons. Since the discovery of photorefractive solitons in 1992, many universal soliton features have been discovered through investigations on photorefractive solitons.[16] On illumination with an incident beam of light, a space charge field is induced in photorefractive materials, due to which the refractive index changes nonlinearly with increase in incident intensity. This is due to the Pockels' effect. This process counteracts the effects of diffraction. Hence, a soliton beam can be formed which propagates without changing its shape due to

an exact balancing between diffraction and self-focusing or defocussing nonlinearity. Currently, many different types of solitons in photorefractive materials have been observed, of which some important ones are quasi-steady state solitons,[17,18] screening solitons,[19–21] photovoltaic solitons,[22–25] screening photovoltaic solitons, etc.[26–28] Screening solitons need the presence of an external bias field. The external bias screens the space charge field nonuniformly and hence, forms an index waveguide which supports the stable propagation of solitons. The photovoltaic solitons can exist in unbiased photorefractive–photovoltaic crystals due to the photovoltaic effect. The bulk photovoltaic effect is responsible for generating the space charge field which in turn creates an index waveguide. Screening-photovoltaic solitons result from the combination of the external bias field and photovoltaic effect.

Now, if two mutually incoherent collinear propagating soliton beams have the same frequency and polarization, they create an effective refractive index modulation due to the combination of their intensities. Each of the soliton beams experiences a refractive index modulation effected by both the beams and hence an incoherently coupled pair is formed. A similar logic can be used to explain incoherently coupled multicomponent solitons in case the incident soliton beams are more than two in number. Incoherently coupled spatial solitons were first investigated theoretically by Christodoulides *et al.*[29] many years ago. They were observed through experimental methods soon after.[30] Since then, incoherently coupled soliton pairs in various realizations have been studied such as screening-photovoltaic solitons, screening solitons and photovoltaic solitons.[31–37] Incoherently coupled multicomponent solitons or soliton families have also been investigated in case of screening photovoltaic solitons in both, the symmetric and hybrid realizations.[31–34]

The net internal field inside the crystal is zero at equilibrium in a ferroelectric crystal. This is because the charge distribution on the crystal faces compensates the field due to spontaneous polarization. In such a crystal, a temperature change causes a spontaneous polarization change and hence, a transient electric field E_{py}. This is called as the pyroelectric field. This field is not compensated immediately and consequently, a drift current can be set up mimicking the effect of an external electric field applied to the crystal. Now, this field is locally screened due to the space charge field formed due to the photorefractive effect and hence, a self-trapped beam results.

Pyroelectric spatial solitons or pyrolitons, originating from the pyroelectric field in photorefractive–photovoltaic crystals have been predicted and observed.[38,39] The theory for spatial solitons in pyroelectric photovoltaic–photorefractive media has also been discussed for open circuit crystals.[40] The writing of soliton waveguides due to the pyroelectric effect in lithium niobate has been discussed in Refs. 41 and 42. Recently, we investigated the effect of pyroelectricity on solitons in biased photovoltaic–photorefractive media.[43] Also, incoherently coupled soliton pairs have been shown to exist theoretically in open circuit photovoltaic–photorefractive crystals along with the pyroelectric effect.[44]

Notable is the fact that[38,38–44] these researches were in photovoltaic–photorefractive crystals. It has been recently predicted that significant pyroelectric effects alone can also support solitons in photorefractive crystals which do not have any bulk photovoltaic effects.[45] In addition, it is emphasized that replacing the external electric field with the temperature change induced pyroelectric field has clear advantages. Firstly, we need not know the direction of the crystal c-axis since the pyroelectric field is always along the c-axis, i.e., in one direction for heating and in the reverse direction for cooling. Secondly, no electrodes are required on the crystal.[41,42] To the best of our knowledge, the coupling of solitons in photorefractive media in which the external electric field is replaced by a temperature induced pyroelectric field has not yet been investigated. In this paper, we formulate the theory for incoherently coupled soliton pairs solely due to the pyroelectric effect in photorefractive crystals. The existence of incoherently coupled soliton pairs in the four realizations, namely, bright–bright, dark–dark, gray–gray, and bright–dark is predicted. The conditions for the formation of each of these soliton pairs are discussed in detail. In addition, the effects of the magnitude of the temperature change and the total beam intensity on the self-trapping of the soliton pairs have been studied.

2. Theory

We shall consider two optical beams propagating collinearly in a photorefractive pyroelectric nonphotovoltaic crystal. We shall consider the diffraction in x-direction only and that the beams are polarized linearly along the x–direction. The crystal is kept between an insulating plastic cover and a metallic plate whose temperature is controlled accurately. As usual, the incident beams are expressed as slowly varying envelopes $\mathbf{E}_1 = \hat{x}A_1(x,z)\exp(ikz)$ and $\mathbf{E}_2 = \hat{x}A_2(x,z)\exp(ikz)$ where $k = k_0 n_e$, $k_0 = \frac{2\pi}{\lambda_0}$. Here, n_e is the unperturbed extraordinary refractive index and λ_0 is the free space wavelength. Under these conditions, the evolution of the optical beams is given by[20,29]

$$\left(i\frac{\partial}{\partial z} + \frac{1}{2k}\frac{\partial^2}{\partial x^2} + \frac{k}{n_e}\Delta n\right) A_j(x,z) = 0; \quad j = 1,2, \tag{2.1}$$

$$\Delta n = -\frac{1}{2}n_e^3 g_{\text{eff}} E_{\text{sc}}, \tag{2.2}$$

where $E_{\text{sc}} = E_{\text{pysc}}$ is the space charge field in the medium resulting from the pyroelectric field and the optical beams' intensity.[45] We note here that the diffusion effect has been neglected. g_{eff} is the effective linear electro-optic coefficient. For nonphotovoltaic–photorefractive crystals, E_{pysc} for steady state (for a time $t \gg t_d$ where t_d is the characteristic Maxwell time) has been derived in detail elsewhere as[45]

$$E_{\text{pysc}} = -E_{\text{py}}\frac{I}{I + I_d}, \tag{2.3}$$

where $E_{\rm py}$ is the transient pyroelectric field and is given by[38]

$$E_{\rm py} = -\frac{1}{\varepsilon_0 \varepsilon_r} \frac{\partial P}{\partial T} \Delta T, \tag{2.4}$$

where $\frac{\partial P}{\partial T}$ is the pyroelectric coefficient and ΔT is the magnitude of the temperature change of the crystal and I_d is the dark irradiance, i.e., the intensity at constant illumination region of the crystal, $I(x \to \infty)$.

From the expression for the space charge field (2.3), we can infer that the value and sign of the space charge field depends upon $E_{\rm py}$ which, in turn, can be varied by the change in temperature, i.e., by the requisite heating, or cooling effects.

The total optical power density for the two mutually incoherent beams can be obtained by adding the two Poynting fluxes

$$I = \frac{n_e}{2\eta_0}(|A_1|^2 + |A_2|^2), \tag{2.5}$$

with $\eta_0 = (\mu_0/\varepsilon_0)^{1/2}$.

Substituting $E_{\rm pysc}$ and Δn in (2.1) and in terms of dimensionless variables, one gets the following equation:

$$iU_\xi + \frac{1}{2}U_{ss} + \beta \frac{(|U|^2 + |V|^2)}{(1 + |U|^2 + |V|^2)} U = 0, \tag{2.6}$$

$$iV_\xi + \frac{1}{2}V_{ss} + \beta \frac{(|U|^2 + |V|^2)}{(1 + |U|^2 + |V|^2)} V = 0, \tag{2.7}$$

where we have written

$$A_1 = \left(\frac{2\eta_0 I_d}{n_e}\right)^{1/2} U \quad \text{and} \quad A_2 = \left(\frac{2\eta_0 I_d}{n_e}\right)^{1/2} V, \quad \xi = \frac{z}{k x_0^2},$$

$$s = \frac{x}{x_0}, \quad U_\xi = \frac{\partial U}{\partial \xi}, \quad U_{ss} = \frac{\partial^2 U}{\partial s^2}, \quad \rho = \frac{I_\infty}{I_d},$$

$$I = I_d |U|^2, \quad \beta = \frac{1}{2}(k_0 x_0)^2 n_e^4 g_{\rm eff} E_{\rm py}.$$

As we can see, the intensity scales with the dark irradiance in these dimensionless coordinates.

3. Results and Discussion

3.1. *Bright soliton pair*

In case of a bright–bright incoherently coupled soliton pair, we express the solutions as

$$U = r^{1/2} y(s) \cos(\theta) \exp(i\upsilon\xi), \tag{3.1}$$

$$V = r^{1/2} y(s) \sin(\theta) \exp(i\upsilon\xi), \tag{3.2}$$

where $r = \frac{I_0}{I_d}$ which stands for the ratio of the maximum intensity to the dark irradiance, ν is a nonlinear shift of the propagation constant, $y(s)$ is a normalized bounded function which satisfies $0 \leq y(s) \leq 1$ and $y(\pm\infty) = 0$, $\dot{y}(0) = 0$, $\dot{y}(\pm\infty) = 0$, $y(0) = 1$, $\ddot{y}(\pm\infty) = 0$ and θ is an arbitrary projection angle.

Substituting (3.1) and (3.2) in (2.6) and (2.7), we get a single equation

$$\frac{d^2y}{ds^2} - 2\upsilon y + 2\beta \frac{ry^3}{1 + ry^2} = 0. \tag{3.3}$$

Integrating (3.3) once

$$\frac{1}{2}\left(\frac{dy}{ds}\right)^2 = \upsilon y^2 - \beta y^2 + \frac{\beta}{r}\log(1 + ry^2) = 0. \tag{3.4}$$

Using the boundary conditions of bright solitons, we have

$$\upsilon = \beta - \frac{\beta}{r}\log(1 + r) \tag{3.5}$$

and we get, substituting the value in (3.4),

$$\frac{1}{2}\left(\frac{dy}{ds}\right)^2 = -\frac{\beta}{r}y^2\log(1 + r) + \frac{\beta}{r}\log(1 + ry^2). \tag{3.6}$$

Integrating once more, we get

$$s = \pm\int_y^1 \left[\frac{2\beta}{r}\{\log(1 + r\tilde{y}^2) - \tilde{y}^2\ln(1 + r)\}\right]^{-1/2} d\tilde{y}. \tag{3.7}$$

The envelope $y(s)$ can be found from (3.7) by straightforward numerical integration. Further, the components of the soliton pair can be found by substituting $y(s)$ in (3.1) and (3.2) by means of a θ-projection. Since $y(s)$ is bounded between 0 and 1, we can see from (3.4) that $\beta > 0$ for keeping the RHS positive. Hence, the condition for bright soliton pair formation is that $\beta > 0$. This means that if the pyroelectric coefficient is negative, then change in temperature $\Delta T > 0$ and if the pyroelectric coefficient is positive, then change in temperature $\Delta T < 0$. We shall consider the SBN crystal for illustration. This is a nonphotovoltaic–photorefractive crystal with a negative pyroelectric coefficient. Hence, we take the following parameters,[45–47] $n_e = 2.35$, $\lambda_0 = 532\,\text{nm}$, $x_0 = 20\,\mu\text{m}$, $g_{\text{eff}} = 237\times10^{-12}\,\text{m/V}$, $\varepsilon_0 = 8.85\times10^{-12}\,\text{F/m}$, $\varepsilon_r = 3400$, $\frac{\partial P}{\partial T} = -3 \times 10^{-4}\,\text{Cm}^{-2}\text{K}-1$ and $r = 10$. For $\Delta T = 10°\text{C}$, $20°\text{C}$, we can arrive at the values for $\beta = 20.1$ and 40.2, respectively. Figure 1 shows the normalized intensities of the bright soliton pair.

For studying the global properties of these bright soliton pairs, we plot the existence curve for the incoherently coupled bright solitons in Fig. 2.

As we see, in Fig. 2, we have plotted the graph on a log-linear scale. The soliton full width at half maximum (FWHM) is a marker of the self-trapping. As the value of r increases, the FWHM decreases till about $r = 1$. For $r > 10$, the FWHM again increases nonlinearly with an increase in r.

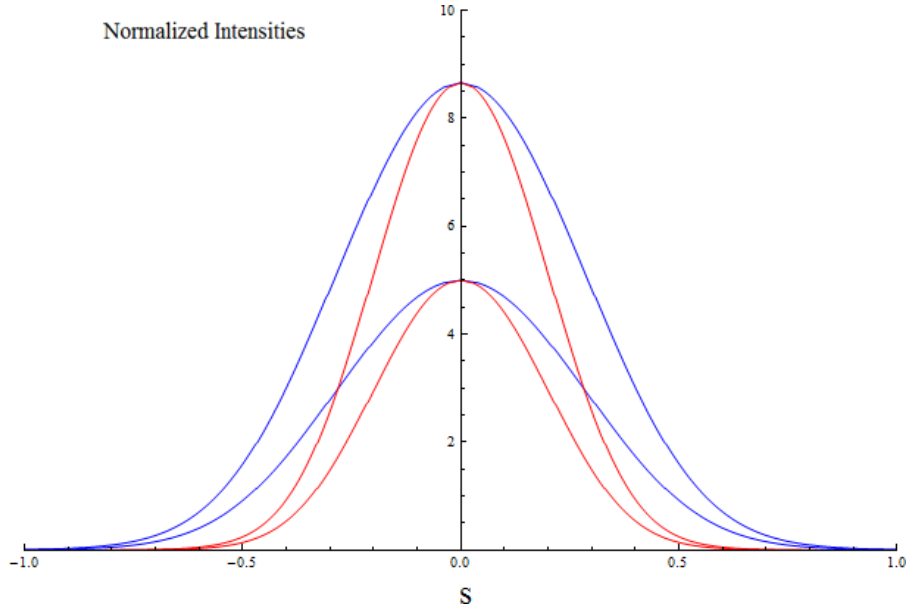

Fig. 1. (Color online) Normalized intensities of the bright incoherently coupled soliton pair under different temperature changes $\Delta T = 10°\text{C}$ (blue) and $\Delta T = 20°\text{C}$ (red) for $r = 10$ and $\theta = \pi/3$.

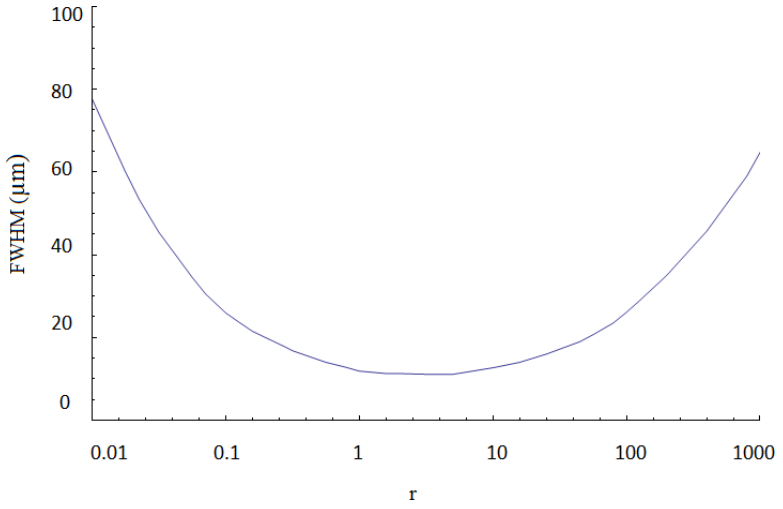

Fig. 2. Existence curve for the incoherently coupled bright pyroelectric soliton pair when $\Delta T = 10°\text{C}$.

3.2. *Dark soliton pair*

In case of a dark–dark incoherently coupled soliton pair, we express the solutions as

$$U = \rho^{1/2} y(s) \cos(\theta) \exp(i\mu\xi), \tag{3.8}$$

$$V = \rho^{1/2} y(s) \sin(\theta) \exp(i\mu\xi), \tag{3.9}$$

where μ is a nonlinear shift of the propagation constant, θ is an arbitrary projection angle, and $y(s)$ is a normalized bounded function which satisfies $0 \leq y(s) \leq 1$ and $y(\pm\infty) = \pm 1$, $\dot{y}(\pm\infty) = 0$, $y(0) = 0$ and $\ddot{y}(\pm\infty) = 0$.

Substituting (3.8) and (3.9) in (2.6) and (2.7), we get a single equation

$$\frac{d^2y}{ds^2} - 2\mu y + 2\beta \frac{\rho y^3}{1 + \rho y^2} = 0. \tag{3.10}$$

Using the boundary conditions of dark solitons, we have

$$\mu = \frac{\beta\rho}{1 + \rho}. \tag{3.11}$$

Integrating (3.10) once

$$\frac{1}{2}\left(\frac{dy}{ds}\right)^2 = \left(\frac{\beta\rho}{1 + \rho}\right) y^2 - \beta y^2 + \frac{\beta}{\rho} \log(1 + \rho y^2) + c, \tag{3.12}$$

where c is a constant of integration. Evaluating the constant of integration c by using the boundary conditions of the dark soliton

$$c = \frac{\beta}{1 + \rho} - \frac{\beta}{\rho} \log(1 + \rho) \tag{3.13}$$

and we get, substituting the value of c in (3.12),

$$\frac{1}{2}\left(\frac{dy}{ds}\right)^2 = \left(\frac{\beta\rho}{1 + \rho}\right) y^2 - \beta y^2 + \frac{\beta}{\rho} \log(1 + \rho y^2) + \frac{\beta}{1 + \rho} - \frac{\beta}{\rho} \log(1 + \rho). \tag{3.14}$$

Integrating (3.14) once more

$$s = \pm \int_y^0 \left[-2\beta \left\{ \frac{\tilde{y}^2 - 1}{1 + \rho} - \frac{1}{\rho} \log\left(\frac{1 + \rho\tilde{y}^2}{1 + \rho} \right) \right\} \right]^{-1/2} d\tilde{y}. \tag{3.15}$$

The envelope $y(s)$ can be found from (3.15) by straightforward numerical integration. Further, the components of the soliton pair can be found by substituting $y(s)$ in (3.8) and (3.9) by means of a θ-projection. Since $y(s)$ is bounded between 0 and 1, we can see from (3.14) that $\beta < 0$ for keeping the right-hand side (RHS) positive. Hence, the condition for bright soliton pair formation is that $\beta < 0$. This means that if the pyroelectric coefficient is negative, then change in temperature $\Delta T < 0$ and if the pyroelectric coefficient is positive, then change in temperature $\Delta T > 0$. In the present illustration as mentioned in Sec. 3.1, since we consider the SBN crystal, for $\Delta T = -10°\text{C}$ and $-20°\text{C}$, we can arrive at the values for $\beta = -20.1$ and -40.2, respectively. Since ΔT is negative, hence the dark soliton

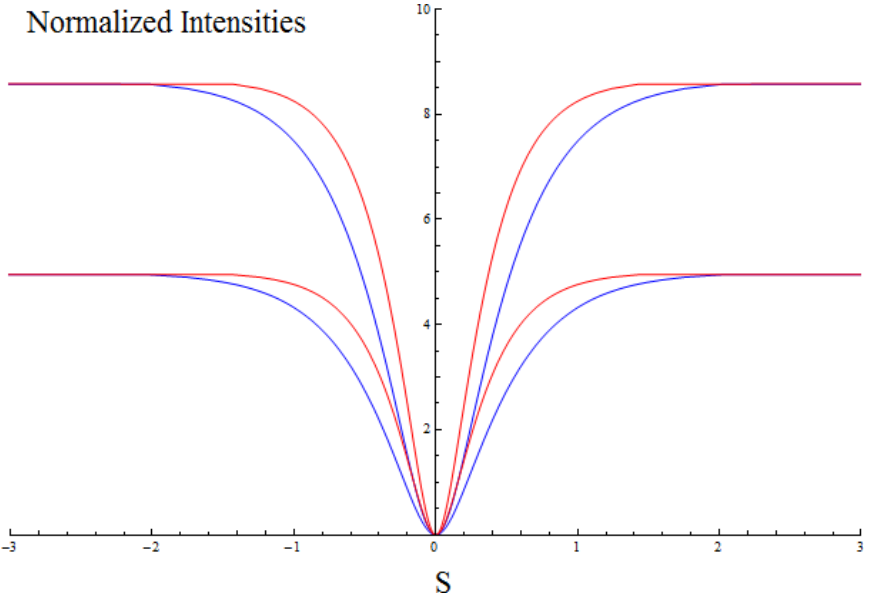

Fig. 3. (Color online) Normalized intensities of the dark incoherently coupled soliton pair under different temperature changes $\Delta T = -10°\text{C}$ (blue) and $\Delta T = -20°\text{C}$ (red) for $\rho = 10$ and $\theta = \pi/3$.

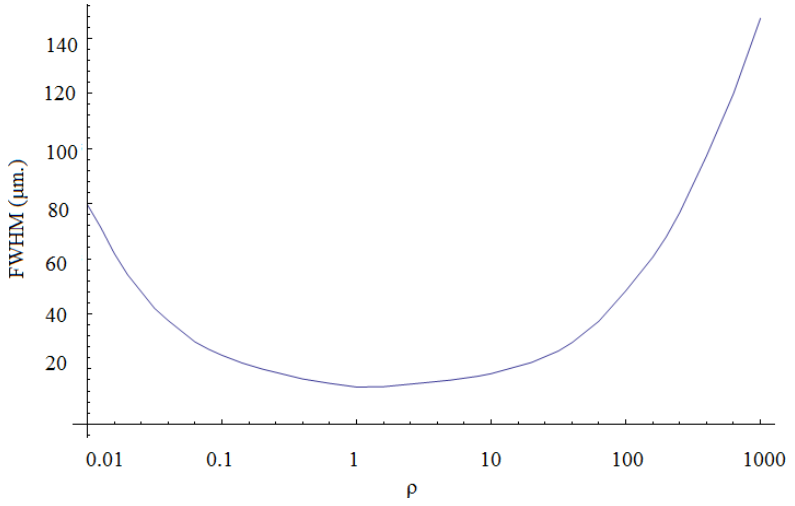

Fig. 4. Existence curve for the dark incoherently coupled pyroelectric soliton pair when $\Delta T = -10°\text{C}$.

pair results from cooling the crystal between the specified temperature difference. Figure 3 shows the normalized intensities of the dark soliton pair.

For studying the global properties of the incoherently coupled dark soliton pair, we plot the existence curve in Fig. 4. From Fig. 4, we can see that the FWHM of

the soliton pair decreases with an increase in ρ for low values of ρ till about $\rho \cong 1$ after which for greater values of ρ, the FWHM rapidly increases.

3.3. *Gray soliton pair*

We express the solutions as

$$U = \rho^{1/2} y(s) \cos(\theta) \exp\left[i\left(\mu\xi + \int_0^s \frac{\Gamma d\tilde{s}}{y^2(\tilde{s})}\right)\right], \tag{3.16}$$

$$V = \rho^{1/2} y(s) \sin(\theta) \exp\left[i\left(\mu\xi + \int_0^s \frac{\Gamma d\tilde{s}}{y^2(\tilde{s})}\right)\right]. \tag{3.17}$$

Substituting (3.16) and (3.17) in (2.10) and (2.11)

$$\ddot{y} = 2\mu y + \frac{\Gamma^2}{y^3} + 2\beta \frac{\rho y^3}{1+\rho y^2} = 0. \tag{3.18}$$

Here, we have the boundary conditions,

$$y(s \to \pm\infty) = 1, \quad \dot{y}(0) = 0, \quad y^2(s=0) = m, \quad \ddot{y}(s \to \pm\infty) = 0.$$

Using the boundary conditions, we get

$$\Gamma^2 = 2\beta \frac{\rho}{1+\rho} - 2\mu, \tag{3.19}$$

$$\mu = \frac{1}{2(m-1)^2}\left\{(1-m)\left(\frac{2\beta\rho}{1+\rho}\right) + \frac{2m\beta}{\rho}\left[\rho(m-1) - \log\left(\frac{1+\rho m}{1+\rho}\right)\right]\right\}. \tag{3.20}$$

Now, integrating (3.18) once and substituting the value of Γ and μ, we get

$$\left(\frac{dy}{ds}\right)^2 = 2\mu(y^2-1) - \Gamma^2\left(\frac{1}{y^2} - 1\right) - \frac{2\beta}{\rho}\left(\rho(y^2-1) - \log\left(\frac{1+\rho y^2}{1+\rho}\right)\right) \tag{3.21}$$

and we can finally find the envelope $y(s)$ by integrating (3.21) once again and substituting the values of μ and Γ

$$s = \pm \int_y^{\sqrt{m}} \left\{2\mu(\tilde{y}^2-1) - \Gamma^2\left(\frac{1}{\tilde{y}^2} - 1\right) - \frac{2\beta}{\rho}\left(\rho(\tilde{y}^2-1) - \log\left(\frac{1+\rho\tilde{y}^2}{1+\rho}\right)\right)\right\}^{-1/2} d\tilde{y}. \tag{3.22}$$

The envelope $y(s)$ can be found from (3.22) by numerical integration. Further, the components of the soliton pair can be found by substituting $y(s)$ in (3.16) and (3.17) by means of a θ-projection. In case of an SBN crystal, as in the case of dark solitons, we need $\beta < 0$. For $\Delta T = -10°\text{C}$ and $-20°\text{C}$, we can arrive at the values for $\beta = -20.1$ and -40.2, respectively. Since ΔT is negative, hence the gray soliton pair results from cooling the crystal between the specified temperature difference. Figure 5 shows the normalized intensities of the gray coupled soliton pair.

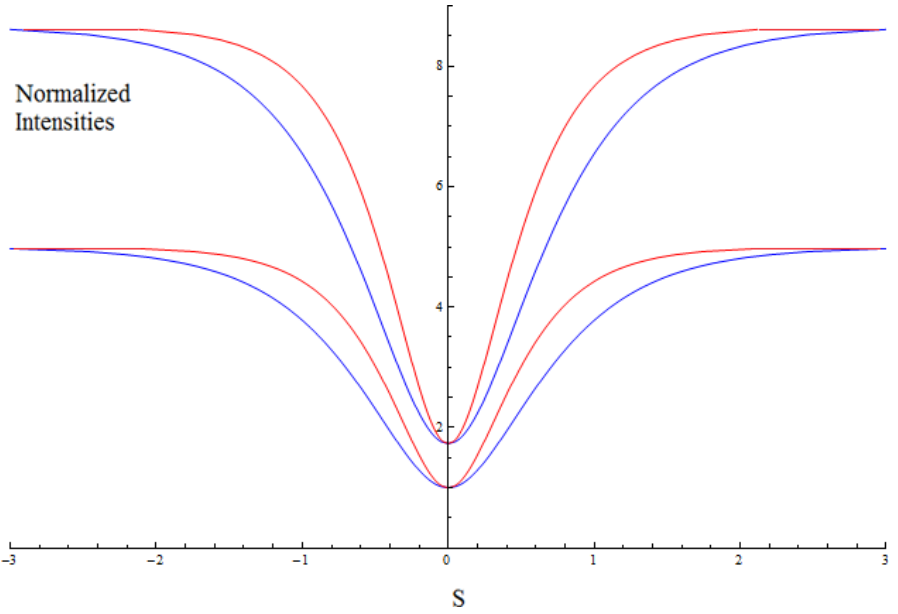

Fig. 5. (Color online) Normalized intensities of the dark incoherently coupled soliton pair under different temperature changes $\Delta T = -10°\text{C}$ (blue) and $\Delta T = -20°\text{C}$ (red) for $\rho = 10$, $m = 0.2$ and $\theta = \pi/3$.

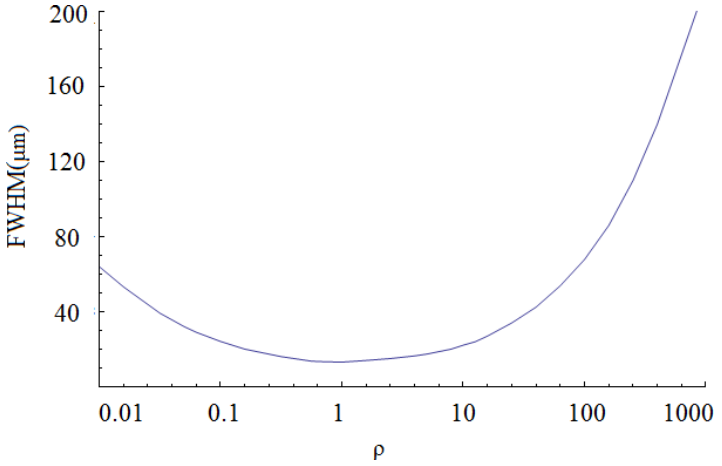

Fig. 6. Existence curve for the incoherently coupled gray pyroelectric soliton pair. $m = 0.2$, $\Delta T = -20°\text{C}$.

For studying the global properties of the incoherently coupled gray soliton pair, we plot the existence curve in Fig. 6.

From Fig. 6, we see that the FWHM of the soliton pair decreases as ρ increases till $\rho \sim 1$ after which the FWHM of the soliton pair rapidly increases with increasing ρ.

3.4. *Bright–dark soliton pair*

We express the two wave envelopes as

$$U = r^{1/2} f(s) \exp(i\mu\xi), \tag{3.23}$$

$$V = \rho^{1/2} g(s) \exp(i\upsilon\xi), \tag{3.24}$$

where μ and ν are the shift in the propagation constants of the bright and dark soliton beams. $f(s)$ is the bright beam and satisfies the boundary conditions $f(0) = 1$, $\dot{f}(0) = 0$, $f(s \to \pm\infty) = 0$. $g(s)$ is the dark beam and satisfies the boundary conditions $g(0) = 0$, $\dot{g}(0) = 0$, $g(s \to \pm\infty) = \pm 1$. Substituting the expressions for U and V in (2.6) and (2.7), we have

$$\frac{d^2 f}{ds^2} = 2\left\{\mu - \beta + \frac{\beta}{1 + rf^2 + \rho g^2}\right\} f, \tag{3.25}$$

$$\frac{d^2 g}{ds^2} = 2\left\{\upsilon - \beta + \frac{\beta}{1 + rf^2 + \rho g^2}\right\} g. \tag{3.26}$$

We put the condition that $f^2 + g^2 = 1$. Thus, we get

$$\frac{d^2 f}{ds^2} = 2\left\{\mu - \beta + \frac{\beta}{1 + \rho}\left(\frac{1}{1 + \sigma f^2}\right)\right\} f, \tag{3.27}$$

$$\frac{d^2 g}{ds^2} = 2\left\{\upsilon - \beta + \frac{\beta}{1 + \rho}\left(\frac{1}{1 + \sigma(1 - g^2)}\right)\right\} g, \tag{3.28}$$

where we have taken

$$\sigma = \frac{r - \rho}{1 + \rho}. \tag{3.29}$$

Integrating (3.27) once

$$\left(\frac{df}{ds}\right)^2 = 2(\mu - \beta)(f^2 - 1) + \frac{2\beta}{\sigma(1 + \rho)} \log\left(\frac{1 + \sigma f^2}{1 + \sigma}\right). \tag{3.30}$$

Using the boundary conditions for $f(s)$ and $g(s)$ in (3.30) and (3.28), respectively,

$$\mu = \beta - \frac{\beta}{\sigma(1 + \rho)} \log(1 + \sigma) \tag{3.31}$$

and

$$\upsilon = \frac{\beta\rho}{(1 + \rho)}. \tag{3.32}$$

If $|\sigma| \ll 1$, then the peak intensities of the two beams are nearly equal. In this limit of $|\sigma| \ll 1$, μ can be expanded by Taylor series and neglecting higher order terms

$$\mu \simeq \beta - \frac{\beta}{1 + \rho}\left(1 - \frac{\sigma}{2}\right). \tag{3.33}$$

Due to $|\sigma| \ll 1$, and substituting (3.32) and (3.33) in (3.27) and (3.28), we have

$$\frac{d^2 f}{ds^2} = \frac{\beta\sigma}{1+\rho}(f - 2f^3), \tag{3.34}$$

$$\frac{d^2 g}{ds^2} = -\frac{2\beta\sigma}{1+\rho}(g - 2g^3). \tag{3.35}$$

Equations (3.34) and (3.35) have a closed form solution

$$f(s) = \operatorname{sech}\left[\left\{\frac{\beta\sigma}{1+\rho}\right\}^{1/2} s\right], \tag{3.36}$$

$$g(s) = \tanh\left[\left\{\frac{\beta\sigma}{1+\rho}\right\}^{1/2} s\right]. \tag{3.37}$$

We can obtain the components of the soliton pair by substituting (3.36) and (3.37) in (3.23) and (3.24)

$$U(s,\xi) = r^{1/2} \operatorname{sech}\left[\left\{\frac{\beta\sigma}{1+\rho}\right\}^{1/2} s\right] \exp\left\{i\beta\left(1 - \frac{1}{1+\rho}\left(1 - \frac{\sigma}{2}\right)\right)\xi\right\}, \tag{3.38}$$

$$V(s,\xi) = \rho^{1/2} \tanh\left[\left\{\frac{\beta\sigma}{1+\rho}\right\}^{1/2} s\right] \exp\left\{i\beta\left(\frac{\rho}{1+\rho}\right)\xi\right\}. \tag{3.39}$$

The FWHM as a function of s can be obtained from (3.38) and (3.39) as

$$\text{FWHM} = \Delta s = 2\log(1+\sqrt{2})\left\{\frac{1+\rho}{\beta\sigma}\right\}^{1/2}. \tag{3.40}$$

From (3.38) and (3.39), we can see that for formation of bright–dark soliton pairs, we must have $\beta(r-\rho) > 0$.

If we take $r > \rho$, that is, the maximum intensity of the respective bright component is slightly larger than the maximum intensity of the respective dark component, then $\beta > 0$ has to be satisfied for the bright–dark soliton pair's existence. In the case of an SBN crystal, this implies that $\Delta T > 0$, which in turn implies a heating of the crystal. On the other hand, if we take $\rho > r$, that is, the maximum intensity of the respective dark component is slightly larger than that of the respective bright component, then we need $\beta < 0$, and hence we have, $\Delta T < 0$, which in turn implies a cooling of the crystal. Thus, we can infer that the bright–dark soliton pair can exist for both, a controlled heating and a controlled cooling of the pyroelectric crystal. Figure 7 shows the normalized intensities of the bright–dark incoherently coupled soliton pair for the case of heating of the crystal, i.e., $\Delta T = 10°\text{C}$ and 20°C.

Figure 8 shows the normalized intensities of the bright–dark incoherently coupled pyroelectric soliton pair for the case of cooling of the crystal, i.e., $\Delta T = -10°\text{C}$ and $-20°\text{C}$.

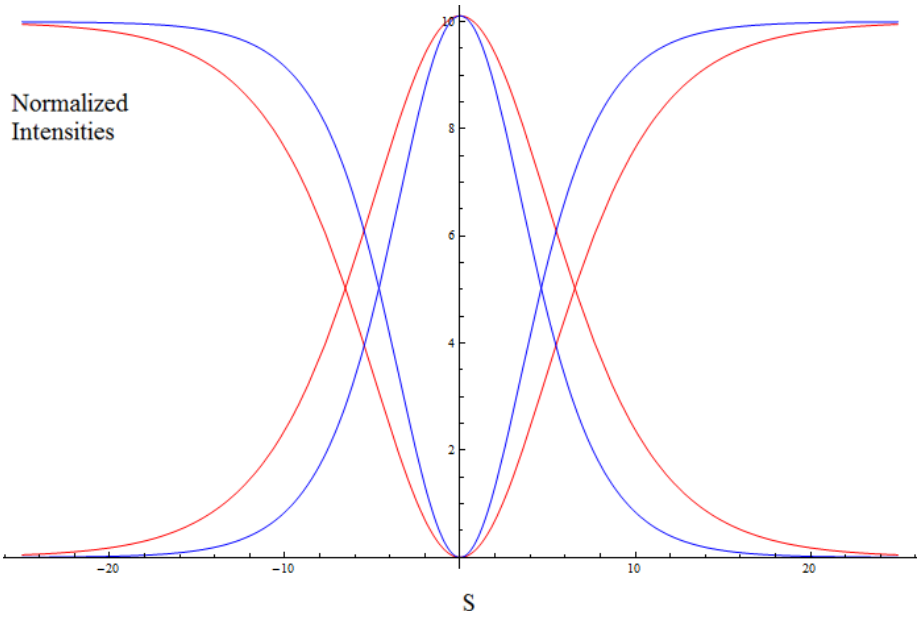

Fig. 7. (Color online) Normalized intensities for the bright–dark incoherently coupled pyroelectric soliton pair for $\Delta T = 10°\mathrm{C}$ (red) and $\Delta T = 20°\mathrm{C}$ (blue), $r > \rho$ and $\rho = 10$.

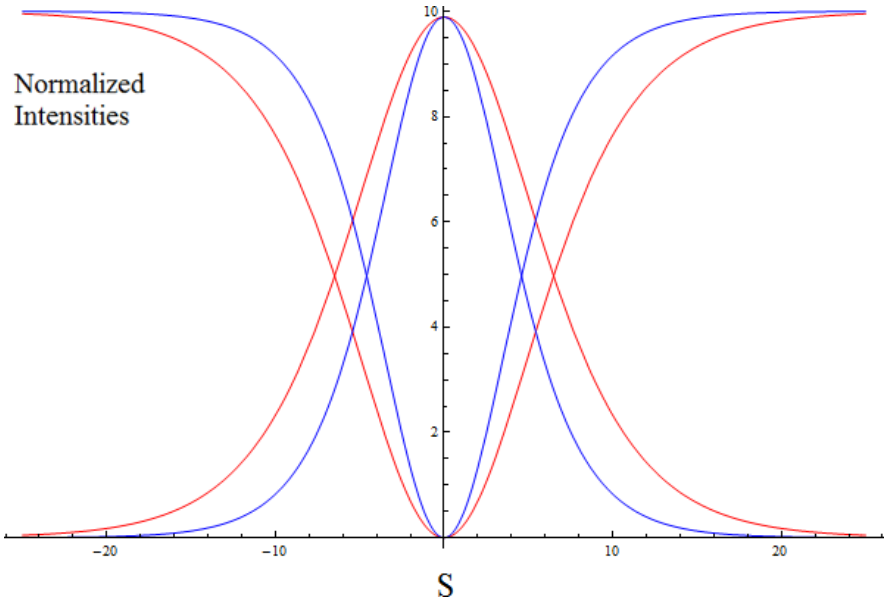

Fig. 8. (Color online) Normalized intensities for the bright–dark incoherently coupled pyroelectric soliton pair for $\Delta T = -10°\mathrm{C}$ (red) and $\Delta T = -20°\mathrm{C}$ (blue), $r < \rho$ and $\rho = 10$.

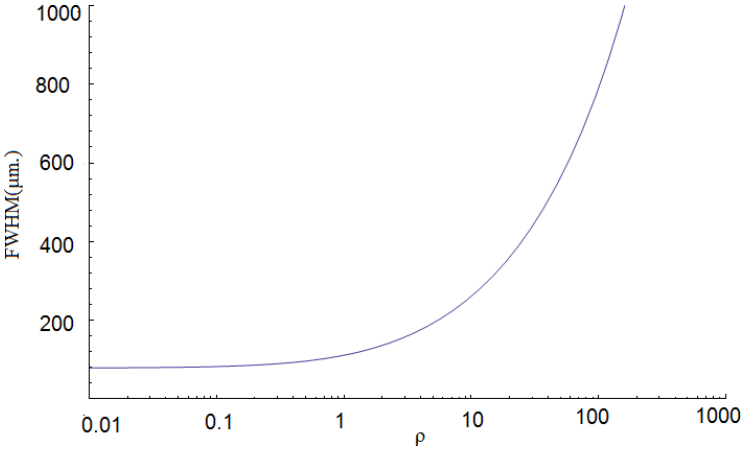

Fig. 9. Existence curve for the bright–dark incoherently coupled bright–dark pyroelectric soliton pair, $\Delta T = -10°\text{C}$.

We plot Eq. (3.40) to obtain the existence curve for the bright–dark incoherently coupled pyroelectric soliton pair for a value of $\sigma = 0.01$. The existence curve is plotted in Fig. 9.

From Fig. 9, we see that the FWHM of the bright–dark incoherently coupled pyroelectric soliton pair remains relatively constant for low values of ρ, which is the maximum intensity of the dark soliton component, and increases with increase of ρ for $\rho > 1$. Interestingly, the FWHM of the bright–dark soliton pair depends upon both r and ρ, the maximum intensity of bright soliton component and dark soliton component, respectively.

4. Conclusion

Hence, to summarize, we have predicted the existence of four types of incoherently coupled soliton pairs, namely, bright–bright, dark–dark, gray–gray, and bright–dark, due to only the pyroelectric effects in photorefractive pyroelectric nonphotovoltaic crystals. The existence of incoherently coupled bright–bright soliton pair requires a heating of the crystal, while the existence of incoherently dark–dark and gray–gray soliton pairs requires a cooling of the crystal. The bright–dark soliton pair can exist for both heating and cooling of the crystal. The FWHM of the bright, dark, gray and bright–dark soliton pairs depends upon the intensity of each soliton component incident upon the crystal.

We would like to mention here that our work is considerably different from some of the recent works on optical solitons.[1–13] Firstly, we consider optical spatial solitons in a photorefractive crystal in our investigation. The solitons in photorefractive media are supported by a saturable nonlinearity. In addition, we study the coupling of two solitons in a photorefractive crystal which has an appreciable pyroelectric coefficient. Also, if we compare the previous researches on coupled spatial soliton

pairs in photorefractive media in particular,[14,15,31–37] we see that the space charge field induced solely due to the transient pyroelectric field differs significantly from the case of screening or screening-photovoltaic solitons and hence, the coupling of solitons in this case is governed by a different theoretical model. We have also elucidated the clear advantages of replacing the external electric field with the temperature induced pyroelectric field for observing soliton coupling in photorefractive materials and hence the motivation behind this investigation.

Acknowledgments

This research was supported through a fellowship awarded by the University Grants Commission, New Delhi awarded to Aavishkar Katti.

References

1. M. Peccianti *et al.*, All-optical switching and logic gating with spatial solitons in liquid crystals, *Appl. Phys. Lett.* **81**(18) (2002) 3335–3337.
2. Y. V. Kartashov *et al.*, Spatial soliton switching in quasi-continuous optical arrays, *Opt. Lett.* **29**(7) (2004) 766–768.
3. T.-T. Shi and C. Sien, Nonlinear photonic switching by using the spatial soliton collision, *Opt. Lett.* **15**(20) (1990) 1123–1125.
4. G. Assanto, N. F. Smyth and W. Xia, Refraction of nonlinear light beams in nematic liquid crystals, *J. Nonlinear Opt. Phys. Mater.* **21** (2012) 1250033.
5. W. Królikowski and Y. S. Kivshar, Soliton-based optical switching in waveguide arrays, *J. Opt. Soc. Am. B* **13**(5) (1996) 876–887.
6. G. Assanto, C. Umeton, M. Peccianti and A. Alberucci, Nematicons and their angular steering, *J. Nonlinear Opt. Phys. Mater.* **15** (2006) 33–42.
7. A. A. Sukhorukov, S. Shoji, Y. S. Kivshar and S. Kawata, Self-written waveguides in photosensitive materials, *J. Nonlinear Opt. Phys. Mater.* **11**(4) (2002) 391–407.
8. A. S. Perin, V. Yu Ryabchenok and V. M. Shandarov, Waveguide circuits formed in lithium niobate samples by bright spatial optical solitons, *2016 Joint IEEE Int. Symp. Applications of Ferroelectrics, European Conference on Application of Polar Dielectrics, and Piezoelectric Force Microscopy Workshop* (*ISAF/ECAPD/PFM*), 21–25 August 2016.
9. A. H. Bhrawy, A. A. Alshaery, E. M. Hilal, W. N. Manrakhan, M. Savescu and A. Biswas, Dispersive optical solitons with Schrödinger–Hirota equation, *J. Nonlinear Opt. Phys. Mater.* **23**(01) (2014) 1450014.
10. H. Kumar and F. Chand, Dark and bright solitary wave solutions of the higher order nonlinear schrodinger equation with self-steepening and self-frequency shift effects, *J. Nonlinear Opt. Phys. Mater.* **22**(01) (2013) 1350001.
11. C. J. Castro and D. Urzagasti, Seesaw drift of bright solitons of the nonlinear Schrödinger equation with a periodic potential, *J. Nonlinear Opt. Phys. Mater.* **25** (2016) 1650038.
12. F. J. Diaz-Otero and P. Chamorro-Posada, Multichannel soliton collisions in strongly dispersion managed WDM transmission systems, *J. Nonlinear Opt. Phys. Mater.* **21** (2012) 1250034.
13. P. Chamorro-Posada and G. S. McDonald, Time domain analysis of Helmholtz soliton propagation using the TLM method, *J. Nonlinear Opt. Phys. Mater.* **21** (2012) 1250031.

14. A. Katti and R. A. Yadav, Coupled spatial solitons in photorefractive multiple quantum well planar waveguides, *Int. Conf. Fibre Optics and Photonics*, OSA Technical Digest (online) (Optical Society of America, 2016), paper Tu3D.3.
15. A. Katti and R. A. Yadav, Coupling effects for grey separate spatial solitons in a biased series photorefractive crystal circuit with both the linear and quadratic electro-optic effects, *Opt. Quantum Electron.* **49**(1) (2017) 36:1–9.
16. P. Gunter, J. P. Huignard (eds.), *Photorefractive Materials and Their Applications I and II* (Springer New York, 2006).
17. M. Segev, B. Crosignani, A. Yariv and B. Fischer, Spatial solitons in photorefractive media, *Phys. Rev. Lett.* **68** (1992) 923–926.
18. G. C. Duree, J. L. Shultz, G. J. Salamo, M. Segev, A. Yariv, B. Crosignani, P. Di Porto, E. J. Sharp and R. Neurgaonkar, Observation of self-trapping of an optical beam due to the photorefractive effect, *Phys. Rev. Lett.* **71** (1993) 533–536.
19. M. Segev, G. C. Valley, B. Crosignani, P. Di Porto and A. Yariv, Steady-state spatial screening solitons in photorefractive materials with external applied field, *Phys. Rev. Lett.* **73** (1994) 3211–3214.
20. D. N. Christodoulides and M. I. Carvalho, Bright, dark, and gray spatial soliton states in photorefractive media, *J. Opt. Soc. Am. B* **12** (1995) 1628–1633.
21. A. G. Grandpierre, D. N. Christodoulides, T. N. Coskun, M. Segev and Y. S. Kivshar, Gray spatial solitons in biased photorefractive media, *J. Opt. Soc. Am. B* **18** (2001) 55–63.
22. G. C. Valley, M. Segev, B. Crosignani, A. Yariv, M. M. Fejer and M. C. Bashaw, Dark and bright photovoltaic spatial solitons, *Phys. Rev. A* **50** (1994) R4457–R4460.
23. M. Taya, M. C. Bashaw, M. M. Fejer, M. Segev and G. C. Valley, Observation of dark photovoltaic spatial soliton, *Phys. Rev. A* **52** (1995) 3095–3100.
24. M. Segev, G. C. Valley, M. C. Bashaw, M. Taya and M. M. Fejer, Photovoltaic spatial solitons, *J. Opt. Soc. Am. B* **14** (1997) 1772–1781.
25. W. L. She, K. K. Lee and W. K. Lee, Observation of two-dimensional bright photovoltaic spatial solitons, *Phys. Rev. Lett.* **83** (1999) 3182–3185.
26. J. Liu and K. Lu, Screening-photovoltaic spatial solitons in biased photovoltaic–photorefractive crystals and their self-deflection, *J. Opt. Soc. Am. B* **16** (1999) 550–555.
27. J. Liu and Z. Hao, Evolution of separate screening soliton pairs in a biased series photorefractive crystal circuit, *Phys. Rev. E* **65** (2002) 066601.
28. K. Lu, T. Tang and Y. Zhang, One-dimensional steady-state spatial solitons in photovoltaic photorefractive materials with an external applied field, *Phys. Rev. A* **61** (2000) 053822.
29. D. N. Christodoulides, S. R. Singh, M. I. Carvalho and M. Segev, Incoherently coupled soliton pairs in biased photorefractive crystals, *Appl Phys. Lett.* **68**(13) (1996) 1763–1765.
30. Z. Chen, T. H. Coskun, D. N. Christodoulides and M. Segev, Observation of incoherently coupled photorefractive spatial soliton pairs, *Opt. Lett.* **21**(18) (1996) 1436–1438.
31. S. Konar, S. Jana and S. Shwetanshumala, Incoherently coupled screening photovoltaic spatial solitons in biased photovoltaic photorefractive crystals, *Opt. Commun.* **273** (2007) 324–333.
32. H. Chun-Feng, L. Bin, S. Xiu-Dong, J. Yong-Yuan and X. Ke-Bin, Incoherently coupled screening-photovoltaic soliton families in biased photovoltaic photorefractive crystals, *Chin. Phys.* **10** (2001) 310.
33. L. Keqing, Z. Yanpeng, T. Tiantong and L. Bo, Incoherently coupled steady-state soliton pairs in biased photorefractive–photovoltaic materials, *Phys. Rev. E* 64 (2001) 056603:1–9.

34. C. Hou, Z. Zhou, X. Sun and B. Yuan, Incoherently coupled gray–gray screening-photovoltaic soliton pairs in biased photovoltaic-photorefractive crystals, *Optik* **112** (2001) 17–20.
35. C. Hou, Y. Pei, Z. Zhong-Xiang and X. Sun, Bright–dark incoherently coupled photovoltaic soliton pair, *Chin. Phys.* **14** (2005) 349–352.
36. H. Wang and X. Peng, Incoherently coupled soliton pairs in photovoltaic crystals, *Chin. J. Phys.* **50** (2012) 589–597.
37. L. Keqing, Z. Wei, Y. Yanlong, C. Guangde, X. Jingjun, Z. Yanpeng and H. Xun, Incoherently coupled gray–gray soliton pairs in biased photorefractive–photovoltaic crystals, *Opt. Mater.* **27** (2005) 1845.
38. J. Safioui, F. Devaux and M. Chauvet, Pyroliton: Pyroelectric spatial soliton, *Opt. Exp.* **17**(24) (2009) 22209–22216.
39. J. Safioui, E. Fazio, F. Devaux and M. Chauvet, Surface-wave pyroelectric photorefractive solitons, *Opt Lett.* **35**(8) (2010) 1254–1256.
40. Q. Jiang, Y. Su and X. Ji, Pyroelectric photovoltaic spatial solitons in unbiased photorefractive crystals, *Phys. Lett. A* **376**(45) (2012) 3085–3087.
41. S. T. Popescu, A. Petris and V. I. Vlad, Fast writing of soliton waveguides in lithium niobate using low-intensity blue light, *Appl. Phys. B* **108**(4) (2012) 799–805.
42. S. T. Popescu, A. Petris and V. I. Vlad, Recording of self-induced waveguides in lithium niobate at 405 nm wavelength by photorefractive–pyroelectric effect, *J. Appl. Phys.* **113**(21) (2013) 213110–213120.
43. A. Katti and R. A. Yadav, Spatial solitons in biased photovoltaic photorefractive materials with the pyroelectric effect, *Phys. Lett. A* **381**(3) (2017) 166–170.
44. Y. Su, Q. Jiang and X. Ji, Incoherently coupled photorefractive spatial soliton pairs based on the combination of pyroelectric and photovoltaic effect, *Acta. Photonica. Sin.* **3** (2014) 014.
45. Y. Su, Q. Jiang and X. Ji, Photorefractive spatial solitons supported by pyroelectric effects in strontium barium niobate crystals, *Optik* **126** (2015) 1621–1624.
46. K. Kos, H. X. Meng, G. Salamo, M. F. Shih, M. Segev and G. C. Valley, One-dimensional steady-state photorefractive screening solitons, *Phys. Rev. E* **53**(5) (1996) R4330–R4333.
47. A. A. Savchenkov, A. B. Marsko, V. S. Ilchenko, I. Solomatine, D. Seidel and L. Maleki, RF-induced change of optical refractive index in strontium barium niobate, *Proc. SPIE* **8600** (2013) 86000O.